Rev. Roum. Sci. Techn.– Électrotechn. et Énerg.
Vol. **70**, *2*, pp. 235–240, Bucarest, 2025

Automatique et ordinateurs
Automatics and computers

WIND TURBINE PITCH ANGLE CONTROL WITH ARTIFICIAL NEURAL NETWORKS

HALIL EROL, ATAKAN ARSLAN

Keywords: Wind turbine; Artificial neural networks; Adaptive neuro-fuzzy inference systems (ANFIS); Pitch angle control.

Pitch angle control in wind turbines is required to obtain maximum efficiency from wind turbines at variable wind speeds. Since the wind turbine pitch control structure is not linear, the control cannot be fully achieved, and oscillations occur at the power output. This oscillation can increase because the pitch angle cannot be adjusted stably. This study employs pitch angle control using artificial neural networks, a proportional-integral-derivative (PID) controller, and adaptive neuro-fuzzy inference systems (ANFIS) methods. When the artificial neural network, PID, and ANFIS outputs are compared, it is evident that the system created using the artificial neural network yields better results than the PID. However, the best output is obtained with ANFIS pitch angle control. Two types of performance indices are used in the performance comparison: the error performance indices and the time response performance indices. Considering the control performance parameters, the maximum overshoot of the PID-controlled system is 0.68 %, while the maximum overshoot of the artificial neural network-controlled system is 0.48 %. The maximum overshoot of the ANFIS-controlled system is 0.46%. As a result, better system performance and a more stable power output are obtained compared to the studies in the literature.

1. INTRODUCTION

Today, it is observed that access to fossil fuels has become more difficult due to various political tensions, and therefore, the costs of using these resources have increased. Also, climate change is another challenge that we must overcome. It is a historical fact that similar energy crises have been experienced in the past. To mitigate the impact of these energy crises, it is essential to increase the use of alternative, sustainable energy sources. One of the sustainable energy sources is wind energy. One method for generating power from wind energy involves the use of wind turbines.

The amount of electricity produced by a wind turbine is generally related to the size of the wind turbine and its components [1,2]. For example, a larger blade sweep area results in more output power. In addition, the most critical factor affecting wind turbines' output power is the wind speed coming to the wind turbine [3,4]. Wind speed is an essential factor in determining the location of wind turbines. Depending on the wind speed, the operating regions of the wind turbines are defined [5]. In these regions, the mode in which the wind turbine will operate was determined. This is also called the wind-power curve. A power curve shows how the power of a wind turbine changes with wind speed. Variable speed variable blade angle wind turbines have three different operation zones. This raises three distinct situations or regions that require attention. In zone 1, the wind speed(Ω) is lower than the wind speed needed for the wind turbine to activate, and the wind turbine is kept closed until the wind speed reaches a certain speed. In other words, wind turbines do not operate in this region and are at a standstill. In region 2, the wind speed(Ω) is between the turbine operating wind speed and the nominal power wind speed(Ωs). The wind turbine is operational in this region, and the blade angle is not controlled. In zone 3, the wind speed is controlled to supply a continuous rated output. This region refers to the area up to the maximum wind speed at which the wind turbine pitch should be controlled. As seen in Fig. 1, no matter how much the wind speed in this region increases, constant power is always observed at the output. However, to prevent excessive wind speed loading in this region, the system is turned off and disabled when it is above a specific value (1.3 $\Omega s \geq \Omega$). This part is shown in Fig. 1 as a 4th region. Since the wind speed is variable in zone 3, blade angle control becomes essential to obtain a constant power output. The blade angle, zero in zone 2, must be at a nominal value in zone 3. Thanks to the servo motors on the blades, the blade angle can be adjusted by rotating the blades. The controller determines the amount of rotation and when it will occur. These regions are shown in Fig. 1 as region 1, region 2, region 3, and region 4.

Various methods can adjust wing position. Pitch angle can be controlled using artificial neural networks (ANN), fuzzy logic control (FLC), optimization, PID systems, and even by combining these systems. Numerous studies in the literature utilize artificial neural networks [6–12]. In the study by Tiwari et al., blade angle control was employed to regulate the wind energy conversion system [13]. The permanent magnet synchronous generator (PMSG) used in the system is a 2 MW wind turbine. It is stated that the proposed controller has approximately 2%, 5%, and 9.5% more power output at the wind-rated speed than the backpropagation neural network, FLC, and PI, respectively.

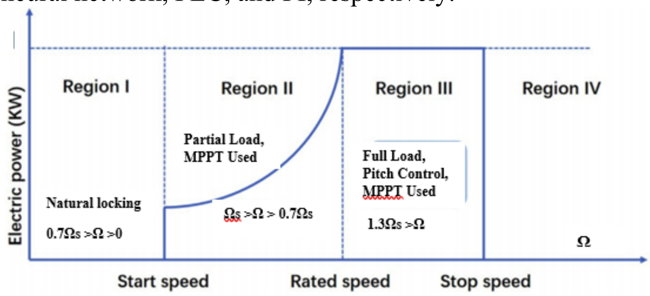

Fig. 1 – Wind turbine operating regions.

In another 2 MW wind turbine study, an attempt was made to adjust the pitch angle with a Radial Basis Function Network (RBFNN) and a Multilayer Perceptron Neural Network (MLPNN) [14]. In this study, a multi-layer perceptron artificial neural network was used. The multi-layer perceptron artificial neural network gave much more successful results compared to a PID-type control. Error rates were almost half those of the PID. In an uncontrolled state, the system turns itself off by exceeding a certain power.

It was stated that RBFNN reached stability earlier than MLPNN. Dahbi et al. [15] conducted a study using a 6.6 kW wind turbine system. They used the Leveneberg-Marquardt method. They experimented with an artificial neural network featuring two hidden layers, with cell numbers of 10 and 20,

[1] Engineering Faculty, Department of Electrical and Electronics Engineering, Osmaniye Korkut Ata University, Osmaniye, Türkiye.
E-mails: halilerol@osmaniye.edu.tr; atakanarslan@osmaniye.edu.tr

DOI: 10.59277/RRST-EE.2025.2.14

respectively. The output obtained using the Levenberg-Marquardt method shows good performance at the optimal rotor speed.

A radial basis artificial neural network is used to control the pitch angle of a 5 MW turbine [16]. As a result of the studies, although power oscillations were observed, it was found that artificial neural networks were more successful than the PI control.

In another study, an adaptive controller is designed for variable speed, variable blade angle wind turbines. A synthesis of the Nussbaum-type function and adaptive radial basis function neural network is proposed to protect the output power against disturbances from unknown sources and to prevent fluctuations. The blade angle is given as input to the neural network while the generator torque is kept at its nominal value. Finally, the performance of the proposed controller is compared with that of a PI controller and a new adaptive method through simulations. The simulation results confirmed the analytical results regarding the stability of the closed-loop system. Moreover, the proposed controller outperformed both the PI Controller and the existing adaptive method [17].

Ernesto et al. [18] use a teaching-learning-based optimization algorithm in pitch angle control for small wind farms constructed in areas with high wind speed variation. The wind speed and its magnitude variation are used to determine PI controller gain parameters. The algorithm is stated to have a rapid calculation time, lower overshoot, and reduced stabilization period under various wind disturbances.

Deep learning and fuzzy logic methods are also used in the pitch angle control of wind turbines [19]. Practical wind speed estimation and prediction are achieved using deep learning neural networks. This value is used in FLC as an input. It is found that a 21 % improvement is obtained concerning the PID controller.

A hybrid intelligent learning based adaptive neuro-fuzzy algorithm is used to schedule the pitch angle of a variable-speed wind turbine, which has 2 MW of rated power. The parameters of fuzzy membership functions (MFs) are trained by the artificial neural network (ANN). In forward pass training, the least squares estimator is used, while in backward pass, the back propagation gradient descent method is used [20]. It is stated that, in terms of accuracy used neuro-fuzzy algorithm has attained good results with least RMSE and MSE measures.

A PID controller with automatic gain adjustment using a fuzzy logic controller (FLC) is introduced in an article [18]. In this study, FLC membership functions are determined by measuring wind speed at some calculated distances, wind variability statistics, and wind path dynamic analysis. The response of the actuator is predicted before the arrival of the wind to the rotor. In another study, a wind turbine pitch controller was designed and implemented using offline fuzzy model-predictive control. They stated that their proposed system guarantees the stability of the wind turbine generator with actuator and linear matrix inequality constraints [21].

2. MODELLING OF WIND TURBINE

Different wind turbine models are used in the literature. The overall block diagram of analysed wind turbine is shown in Fig. 2 [22–24]. The modelling of wind turbines is essential for designing efficient and reliable wind energy systems, evaluating different control strategies, conducting performance simulations, and optimizing wind farm layouts.

The power produced from the wind turbine depends on the wind speed (v), the power coefficient (Cp), the blade swept area (A), and the air density (ρ). The formula for calculating the power output of wind energy conversion systems is stated in eq. (1). The wind turbine output power function, in which factors such as wind energy coming to the turbine rotor, turbine swept area, and air density are affected as given in eq. (1). The moment transferred to the shaft is expressed in eq. (2),

$$P_t = 0.5\, A\, p\, C_p(\beta,\lambda)\, v^3 \ \text{[W]}, \tag{1}$$

$$T_t = 0.5\, A * p * \left(\frac{C_p(\beta,\lambda)}{\lambda}\right) v^2 \ \text{[Nm]}. \tag{2}$$

P_t refers to the output power obtained from the turbine, p is air density(p=1.225), Cp is the power coefficient, A (=πr^2) is the rotor swept area, β is the wing angle, and λ is the tip velocity ratio. The power coefficient for this study is taken as follows:

$$C_p(\lambda,\beta) = 0.5176\left(\frac{116}{\lambda_i} - 0.4\beta - 5\right) e^{-\frac{21}{\lambda_i}} + 0.0068\lambda, \tag{3}$$

$$\frac{1}{\lambda_i} = \left(\frac{1}{\lambda+0.08\beta} - \frac{0.035}{3\beta+1}\right). \tag{4}$$

The tip velocity ratio λ in eq. (3) is,

$$\lambda = \frac{w_t R}{v} \tag{5}$$

w_t is the turbine speed, and R is the rotor blade length.

3. MODELLING OF CONTROL SYSTEMS

Classic PID controllers are widely employed in control systems because their structure is simple and can be easily realized [25]. However, wind turbines are strongly nonlinear systems, so a linear PID controller cannot meet the system's requirements. Typically, the PID algorithm is combined with an intelligent algorithm to create a new controller that can achieve significantly improved control performance.

Since wind turbine output is proportional to the cube of wind speed, produced wind energy is not constant. For this reason, the power output of wind turbine fluctuates. As can be seen from the wind turbine modelling section, the wind turbine is a nonlinear system. To improve power quality and maintain the stable output generated by a wind turbine, this paper presents a pitch controller mechanism based on three types of controllers: artificial neural networks, PID controllers, and ANFIS, for smoothing output power fluctuations.

3.1 PID MODELLING

The classical method of pitch angle control is the proportional integral derivative (PID), which is based on a mathematical model of the system with feedback of the controlled variable, as it calculates the error between the measured and desired values [6]. To adjust the controller, the weights of the proportional constant, the integral time, and the derivative time (gains) are determined [10]. However, in a variable-speed wind turbine, the optimal response changes as a function of the magnitude of the wind speed variation. This variability makes a PID controller unstable, particularly when subjected to drastic changes in wind speed control. It does not require more labor and complex circuits to work at a reasonable performance [21–26].

The BA block diagram representation of the wind turbine with a PID controller is made using the MATLAB/Simulink software program.

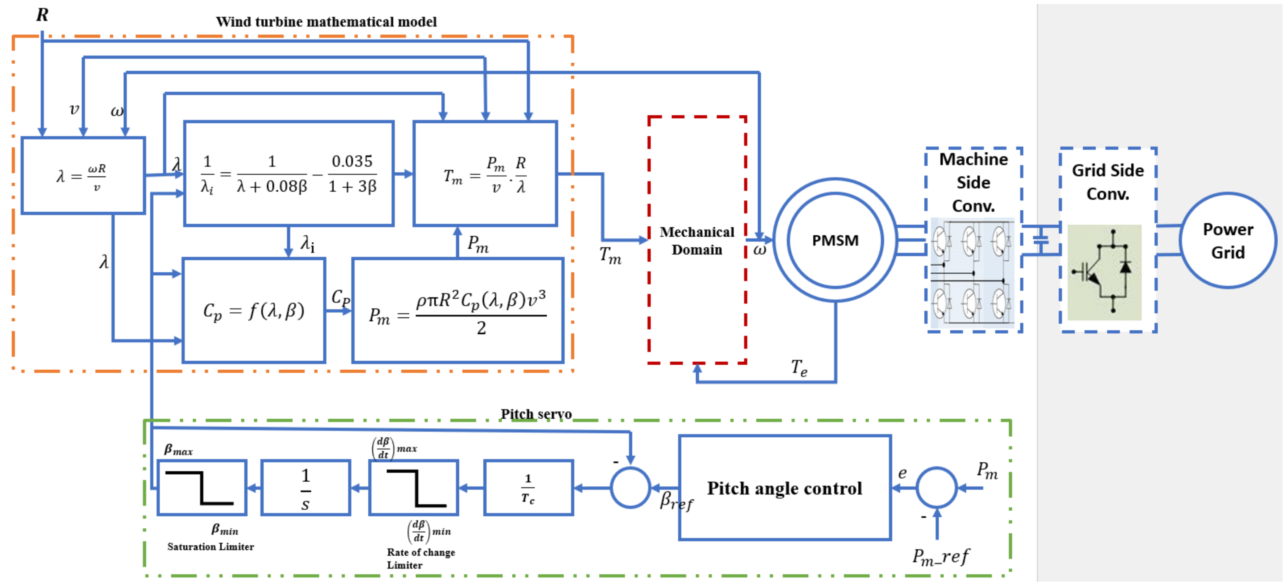

Fig. 2 – Wind turbine overall system block scheme.

As shown in Fig. 3, the PID controller controls the servo motor, which adjusts the blade angle. The wind speed signal applied to the system is a ramp signal. Its magnitude ramps from 0 to 25m/s in 9 s. In this manuscript, six different blade pitch angle control system configurations are designed. Four of these systems are designed with the help of an ANN controller, one with ANFIS, and one with a PID controller. The features of the designed PID system are given in the second section. The features and names of the developed artificial neural network systems are presented in Table 2. The design parameters of ANN systems are specified in Table 3, and ANN results are shown in Table 4. In addition, the output power and characteristic status obtained from each simulation are presented in detail in section 5.

3.2 ARTIFICIAL NEURAL NETWORKS MODELLING

Artificial neural networks are systems that can learn using various algorithms without relying on traditional programming methods. The sigmoid function is widely used in artificial neural networks. In addition, the hyperbolic tangent sigmoid and Purelin functions are also used when creating the artificial neural network architecture [27].

Backpropagation is used for error minimization in artificial neural networks. Input data is propagated forward, and the error between the output and the expected value is calculated. This error is propagated backward to determine its effects on the weights. Finally, the weights are updated using the learning rate. The Purelin function is generally used in the output layer to obtain a linear output in artificial neural networks.

In this study, various activation functions are used in the input and hidden layers. The type of artificial neural networks used in simulations is always a feedback artificial neural network. Feedback artificial neural network is a teacher network. Levenberg-Marquardt feedback function (trainlm), flexible backpropagation function (trainrp), or momentum and adaptive learning rate backpropagation gradient descent function (trainingdx) were chosen as the learning function. The results of each network are tabulated and shown in Table 1. A sample constructed artificial neural network (ANN) model is called YSA6 and is shown in Fig. 5.

3.3 ANFIS MODELLING

The basis of this method is the Takagi-Sugeno-Kang inference system. It aims to minimize error output by adjusting the membership functions in the most effective manner. ANFIS uses gradient descent and a least squares approach with feedback while ensuring the best fit of outputs with given inputs. Membership values are considered in ANFIS systems, which are expected to be set automatically [27,28]. There are inter-layer connection points, and each node represents the entry. These values enter the membership function. Then the rules are normalized. Then the weights are calculated. Finally, all signals are summed up.

ANFIS combines fuzzy logic and neural networks to transform input values into output values. The first layer takes the inputs, while the second layer fuzzifies them using membership functions. The third layer applies fuzzy rules and calculates firing strengths, and the fourth layer normalizes these values. The fifth layer computes the weighted results, and the sixth layer aggregates these results to produce the final output.

4. SIMULATION OF THE SYSTEM MODEL

The created wind turbine and pitch angle control system are obtained with the help of block diagrams in MATLAB Simulink. Simulink block diagram of wind turbine NN control system is shown in Fig. 3. It has three blocks, which are the controller block(NN block), the pitch motor block, and the turbine block.

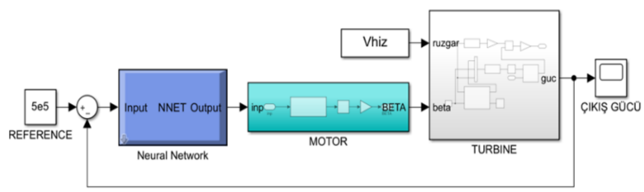

Fig. 3 – Wind turbine NN control system.

The output power of the wind turbine used in the system is 500 kW. It is also chosen as the reference value. The DC servo motor, located on the wind turbine blades, determines the pitch angle. The pitch angle, that is, the Beta(β) value at the output of the DC servo motor, is given as the input value in the wind turbine. The ramp wind speed value can be created with Simulink blocks or pulled from the workspace with the From Workspace block.

Figure 4 shows the internal structure of the wind turbine block. In this internal structure, based on eq. (1), the output power is obtained by using the power coefficient. The power coefficient of the wind turbine is given in eq. (3). The power coefficient is the efficiency of the wind turbine, and it is not fixed [5,18].

The total number of input values used to train artificial neural networks in experiments is 90014. The type of neural networks used in experiments is always a feedback neural network. Levenberg-Marquardt feedback function (trainlm), flexible backpropagation function (trainrp), or Momentum and adaptive learning rate backpropagation gradient descent function (traingdx) are chosen as the learning function.

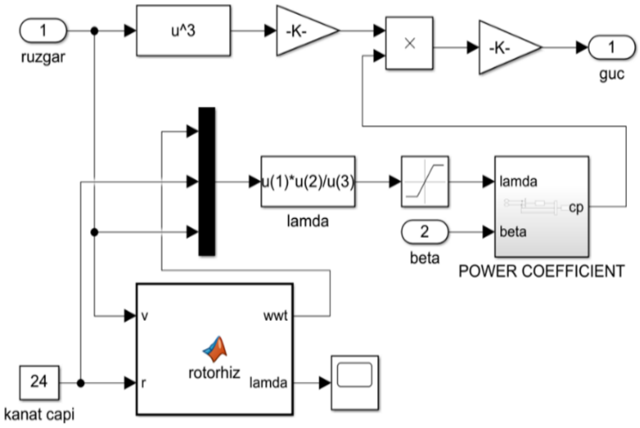

Fig. 4 – Wind turbine block content.

Table 1

Simulation parameters of artificial neural network models.

ANN model	# of Layers	Training Function	Activation Function	# of Epochs
YSA11	3	traingdx	logsig- purelin	2500
YSA6	3	trainlm	tansig-purelin	10000
YSA2	3	trainlm	tansig- purelin	7300
YSA3	3	trainlm	logsig- purelin	7367

In the artificial neural networks created in the experiments, 3-layer networks are preferred. In the output layer of all of them, MATLAB cell and Prelin are chosen as the activation function. The performance function used in networks is mean square error (MSE). Simulation parameters of the artificial neural network models used are shown in Table 1. In all experiments, the artificial neural network consisted of 1 hidden layer. The number of nodes present in the layers is given in Table 2.

Table 2

Neuron numbers(nodes) used in layers.

ANN model Name	Input Layer	Hidden Layer	Output Layer
YSA11	9	9	1
YSA6	9	9	1
YSA2	10	11	1
YSA3	5	5	1

As shown in Table 2, the training functions, epochs, and activation functions used in the experiments vary.

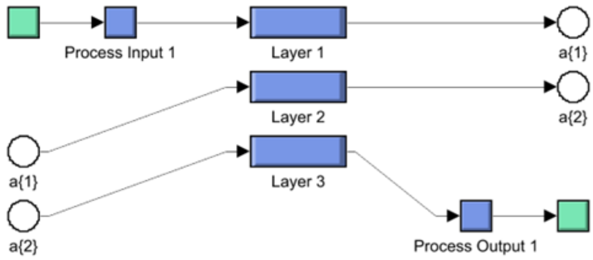

Fig. 5 – Neural network model of the YSA6.

5. RESULTS AND DISCUSSIONS

In this article, a wind turbine system is simulated in MATLAB/Simulink, and the output power is obtained by controlling the simulated wind turbine with artificial neural networks, ANFIS, and PID. The output powers of the designed wind turbine and pitch angle system models are examined. As a result of the studies carried out, the following conclusions are reached. These conclusions are analyzed in an individual subtitle, which is explained below.

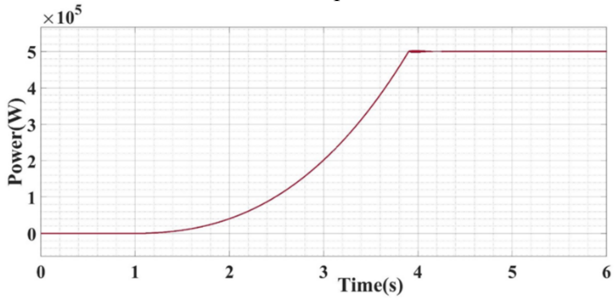

Fig. 6 – Output Power of the wind turbine with PID controller.

5.1 WIND TURBINE OUTPUT POWER VARIATION WITH PID, YSA6, AND YSA11 CONTROLLER

The PID controller block is simulated in MATLAB/Simulink. The proportional gain is -1, and the integrator gain is -0.0001. Derivative coefficient 0 is chosen. The outputs of the PID controller are shown in Fig. 6. In addition, the output power is shown in a zoomed view in Fig. 8. In the system established with PID, the maximum peak point in the appropriate characteristic system, which is created and is reached at 3,965 s. by adjusting the pitch angle and obtained output power is 503.4 kW. The maximum overshoot (MPI) of this system is 0.68%. The output power exhibits small oscillations for a short period and then reaches equilibrium.

In YSA6 model, MATLAB neural network/data manager is used in the artificial neural network, and the Levenberg-Marquardt function is chosen as the training function. NN model of YSA6 is shown in Fig. 5. As the activation function, tansig and purelin are only selected in the output layer. The number of steps is determined as 10000. It is observed that this artificial neural network achieves its maximum point at a power of 503.3 kW, and the maximum overshoot (MYSA6) of this system is 0.66% in percentage terms. However, as seen in Fig. 7, it is not in a balanced and symmetrical image, unlike the system established with PID. The simulated YSA6 reached a stable state almost simultaneously with the system installed with PID. It reaches the steady-state value in 5.31 seconds.

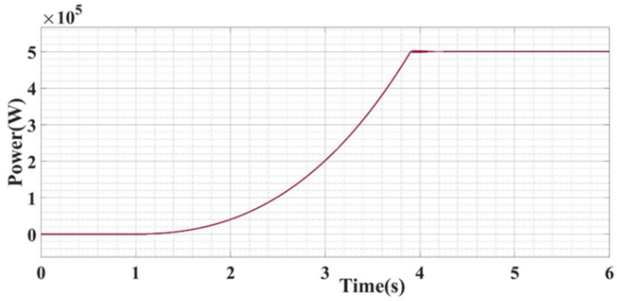

Fig. 7 – Output power of the wind turbine with ANN controller (YSA6 is used).

In the simulation YSA11, which is prepared with the trainingdx training function in MATLAB NN toolbox, logsig is chosen as the activation function, and Purelin function is selected in the output function. The number of steps is determined as 2500. The maximum output power in this simulation is 502.4 kW, achieved in 3.964 seconds, yielding better results compared to the PID results. In addition, better damping is received, as can be seen in Fig. 8. Thus, it is seen that the simulation named YSA11 responds faster than PID. The maximum overshoot of this system is 0.48%.

5.2 WIND TURBINE OUTPUT POWER VARIATION WITH YSA2 AND YSA3 CONTROLLER

In the simulation YSA2, in which the trainingdx training function is used in this artificial neural network, tansig is chosen as the activation function, and purelin function is selected in the output function. The number of steps is determined to be 7,300. The outputs of the YSA2 and YSA3 controllers are shown in Fig. 9. The YSA2 experiment gave a worse result than the experiments created with the artificial neural network, compared to the PID output. As a result of this experiment, it is observed that the value reaches 3.97 s at its maximum. Its maximum value is 508.1 kW. Its maximum overshoot is 1.616%. At 3.962 s, it gives a value as the minimum point, and this minimum value is 496 kW. The value at which output power reaches the steady state is 502.8 kW. The differences with other experiments are more apparent collectively in Table 3.

Table 3

Output power of the wind turbine with the proposed controller and overshoot values

Model Name	Minimum (kW)	Maximum (kW)	maximum overshoot	steady state difference
YSA11	498.133	502.4	%0.48	0.00225
YSA6	498.520	503.3	%0.66	0.00185
PID	496.795	503.4	%0.68	0.00152
ANFIS	497.928	502.3	%0.46	0.00151
YSA2	496.205	508.1	%1.616	0.02808
YSA3	498.267	503.8	%0.755	0.00184

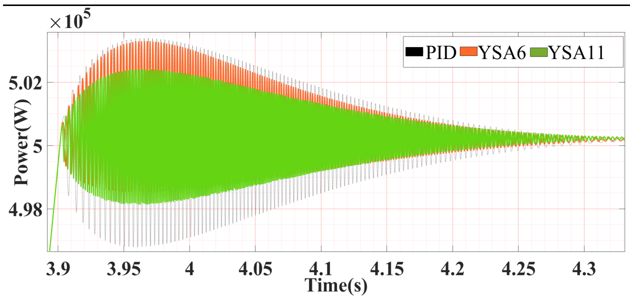

Fig. 8 – The detail view of the output power of the wind turbine with PID, YSA6, and YSA11 controllers.

In YSA3, the Levenberg-Marquardt training function is used. Logsig is used as an activation function, and the Purelin function was used in the last layer. Maximum output power reached at 3.968 seconds and 503.7 kW.

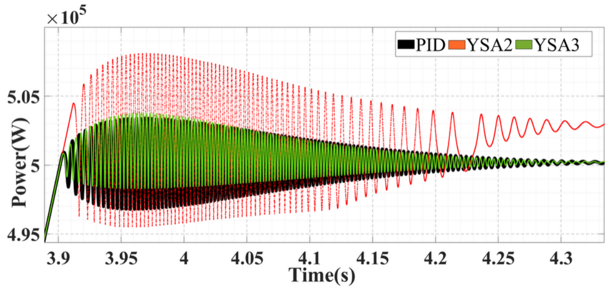

Fig. 9 – Detail view of the output power of the wind turbine with PID, YSA2, and YSA3 controllers.

Its maximum overshoot is 0.755% in percentage. At 3.966 s, it yields a value corresponding to the minimum output power, which is 498.2 kW. The steady-state value of the output power is 500.2 kW. In this case, it can be accepted that it has worse results compared to PID.

5.3 WIND TURBINE OUTPUT POWER VARIATION WITH ANFIS CONTROLLER

The output power obtained when the ANFIS controller is used as a pitch angle controller is shown in Fig. 10. As can be seen from Fig. 10, the output power reaches its maximum value in 3.96 s, which is 502.3 kW. The maximum overshoot is 0.46%. This value stands out as the best value among the experiments. At 3.959 s, it gives a value at the minimum point, and this minimum value is 497.9 kW. The steady-state value of the achieved power is 500.15 kW. In this case, it has better results compared to the PID controller used as a pitch angle controller.

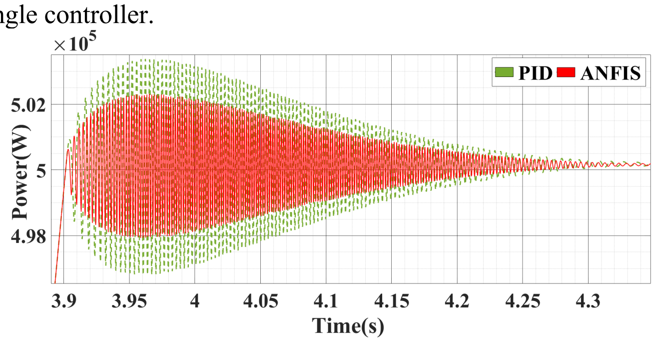

Fig. 10 – Detail view of wind turbine output power graph for ANFIS and PID pitch controller.

Statistical performance indices also analyse outputs of proposed controllers. For comparing the performance of proposed controllers in the considered mission, integral absolute error (IAE), integral squared error (ISE), integral time-weighted absolute error (ITAE), and integral time square error (ITSE) measures have been considered as comparative indices. To evaluate the performance of the proposed controllers, the values of these indices are shown in Table 4.

Table 4

Generator speed response comparisons based on four performance indices for the six regulator models.

Name	IAE	ISE	ITAE	ITSE
YSA11	114.72	$1.78\ 10^{4}$	$1.2\ 10^{3}$	$1.64\ 10^{5}$
YSA6	$4.38\ 10^{5}$	$1.76\ 10^{10}$	$1.44\ 10^{5}$	$4.70\ 10^{10}$
PID	$5.40\ 10^{5}$	$1.86\ 10^{11}$	$1.46\ 10^{6}$	$4.78\ 10^{11}$
ANFIS	113.62	$1.73\ 10^{4}$	$1.0\ 10^{3}$	$1.53\ 10^{5}$
YSA2	$6.61\ 10^{5}$	$1.86\ 10^{11}$	$1.66\ 10^{6}$	$5.80\ 10^{11}$
YSA3	$5.40\ 10^{5}$	$1.86\ 10^{10}$	$1.46\ 10^{6}$	$4.78\ 10^{11}$

The statistical performance indices of the control system with ANFIS yield the smallest error. The second-best one is YSA11.

6. **CONCLUSIONS**

In comparison to previous studies in the literature [6,10], better results are obtained with the ANFIS controller. In addition to the system working well with the PID controller, the experimental simulation of the YSA11 and YSA6 showed that they work more stably in conjunction with the PID controller, providing better output power than the PID controller. While the maximum value of the PID-controlled system is 503 kW, its maximum value is measured as 502.4 kW in the experiment named YSA11. The difference revealed that the system designed with the artificial neural network and utilizing the training function is better, as it has less overshoot. In addition, the wind turbine output results in artificial neural network-supported simulations, named ANN2 and ANN3, which give worse results than the system established with PID. The function used in the experiment named YSA11 is different from the function used while designing ANN2 and ANN3, as shown in Table 3.

It should also be noted that the artificial neural network system created using the trained and login functions gave better results than the artificial neural network controller created using the transit and Levenberg-Marquardt functions. As shown in Table 3, the control system established using ANFIS achieved the best maximum overshoot value and yielded the best output values. Compared to the previous literature studies [28], better results are obtained with the ANFIS controller. It has been demonstrated that the control system employing the ANFIS method achieves the best performance. The control system, with the YSA11 method, generates the second-best performance.

CREDIT AUTHORSHIP CONTRIBUTION STATEMENT

Halil Erol: conceptualization, data curation, methodology, formal analysis, investigation, resources, supervision, validation, writing – review & editing.
Atakan Arslan: formal analysis, investigation, data curation, writing – original draft, visualization.

Received on 3 July 2024

REFERENCES

1. H. Erol, *Stability analysis of pitch angle control of large wind turbines with fractional order PID controller*, Sustainable Energy Grids & Networks, **26** (2021).
2. M. Shoaib, et al, *Assessment of wind energy potential using wind energy conversion system*, Journal of Cleaner Production, **216**, pp. 346–360 (2019).
3. C. Cooney, et al, *Performance characterization of a commercial-scale wind turbine operating in an urban environment, using real data*, Energy for Sustainable Development, **36**, pp. 44–54 (2017).
4. M. El-Ahmar, A.-H. Ahmed, A. Hemeida, *Evaluation of factors affecting wind turbine output power*, pp. 1471–1476 (2017).
5. H. Erol, A. Arslan, *Analysis of wind turbine blade pitch angle control with fuzzy logic*, The International Journal of Materials and Engineering Technology, **5**, *1*, pp. 18–22 (2022).
6. H. Bouregba, et al, *Stability analysis of the pitch angle control of large wind turbines using different controller strategies*, Advances in Mechanical Engineering, **14**, *11*, 16878132221139926 (2022).
7. Z. Civelek, *Optimization of fuzzy logic (Takagi-Sugeno) blade pitch angle controller in wind turbines by genetic algorithm*, Engineering Science and Technology, an International Journal, **23**, *1*, pp. 1–9 (2020).
8. A. Iqbal, et al, *Efficacious pitch angle control of variable-speed wind turbine using fuzzy based predictive controller*, Energy Reports, **6**, pp. 423–427 (2020).
9. A. Lasheen, A.L. Elshafei, *Wind-turbine collective-pitch control via a fuzzy predictive algorithm*, Renewable Energy, **87**, pp. 298–306 (2016).
10. J.E. Sierra-Garcia, M. Santos, R. Pandit, *Wind turbine pitch reinforcement learning control improved by PID regulator and learning observer*, Engineering Applications of Artificial Intelligence, **111**, 104769 (2022).
11. I. Yaichi, S.A. Wira, P. Wira, *Control of doubly fed induction generator using artificial neural network controller*, Rev. Roum. Sci. Techn. – Électrotechn. Et Énerg., **68**, *1*, pp. 46–51 (2023).
12. S. Bellarbi, A.B., *Maximum power wind extraction with feedback linearization control approach*, Rev. Roum. Sci. Techn. – Électrotechn. Et Énerg., **67**, *3*, pp. 237–240 (2022).
13. R. Tiwari, R.Babu.N, *Comparative analysis of pitch angle controller strategies for PMSG based wind energy conversion system*, International Journal of Intelligent Systems and Applications, **9**, pp. 62–73 (2017).
14. A.S. Yilmaz, Z. Ozer, *Pitch angle control in wind turbines above the rated wind speed by multi-layer perceptron and radial basis function neural networks*, Expert Systems with Applications, **36**, *6*, pp. 9767–9775 (2009).
15. A. Dahbi, N. Nait-Said, M.S. Nait-Said, *A novel combined MPPT-pitch angle control for wide range variable speed wind turbine based on neural network*, International Journal of Hydrogen Energy, **41**, *22*, pp. 9427–9442 (2016).
16. H. Jafarnejadsani, J. Pieper, J. Ehlers, *Adaptive control of a variable-speed variable-pitch wind turbine using radial-basis function neural network*, IEEE Transactions on Control Systems Technology, **21**, *6*, pp. 2264–2272 (2013).
17. P. Bagheri, Q. Sun, *Adaptive robust control of a class of non-affine variable-speed variable-pitch wind turbines with unmodeled dynamics*, ISA Transactions, **63**, pp. 233–241 (2016).
18. E. Chavero-Navarrete, et al, *Pitch angle optimization by intelligent adjusting the gains of a PI controller for small wind turbines in areas with drastic wind speed changes*, Sustainability, **11**, *23*, 6670 (2019).
19. J.E. Sierra-Garcia, M. Santos, *Deep learning and fuzzy logic to implement a hybrid wind turbine pitch control*, Neural Computing and Applications, **34**, *13*, pp. 10503–10517 (2022).
20. A.B. Asghar, et al, *Adaptive neuro-fuzzy algorithm for pitch control of variable-speed wind turbine*, International Journal of Control, Automation and Systems, **20**, *11*, pp. 3788–3798 (2022).
21. M.A. Abdelbaky, X. Liu, D. Jiang, *Design and implementation of partial offline fuzzy model-predictive pitch controller for large-scale wind-turbines*, Renewable Energy, **145**, pp. 981–996 (2020).
22. L. Pan, X. Wang, *Variable pitch control on direct-driven PMSG for offshore wind turbine using Repetitive-TS fuzzy PID control*, Renewable Energy, **159**, pp. 221–237 (2020).
23. Y. Xia, et al, *Integrated structure and maximum power point tracking control design for wind turbines based on degree of controllability*, Journal of Vibration and Control, **25**, *2*, pp. 397–407 (2019).
24. B. Boukhezzar, H. Siguerdidjane, *Nonlinear control of a variable-speed wind turbine using a two-mass model*, IEEE Transactions on Energy Conversion, **26**, *1*, pp. 149–162 (2011).
25. H. Erol, *Delay margin computation in micro grid systems with time delay by using fractional order controller*, Electric Power Components and Systems, **49**, *6-7*, pp. 669–680 (2022).
26. Q. Hawari, et al, *A robust gain scheduling method for a PI collective pitch controller of multi-MW onshore wind turbines*, Renewable Energy, **192**, pp. 443–455 (2022).
27. R. Gao, Z. Gao, *Pitch control for wind turbine systems using optimization, estimation and compensation*, Renewable Energy, **91**, pp. 501–515 (2016).
28. E. Hosseini, E. Aghadavoodi, L.M. Fernández Ramírez, *Improving response of wind turbines by pitch angle controller based on gain-scheduled recurrent ANFIS type 2 with passive reinforcement learning*, Renewable Energy, **157**, pp. 897–910 (2020).